

# Spatial Variation of Nuclear Structure Functions and Heavy Quark Production

V. Emel'yanov<sup>1</sup>, A. Khodinov<sup>1</sup>, S. R. Klein<sup>2</sup> and R. Vogt<sup>2,3</sup>

<sup>1</sup>*Moscow State Engineering Physics Institute (Technical University), Kashirskoe ave. 31,  
Moscow, 115409, Russia*

<sup>2</sup>*Nuclear Science Division, Lawrence Berkeley National Laboratory, Berkeley, CA 94720, USA*

<sup>3</sup>*Physics Department, University of California, Davis, CA 95616, USA*

## Abstract

We explore how nuclear modifications to the free nucleon structure functions (also known as shadowing) affect heavy quark production in collisions at different impact parameters. We assume that the nuclear modifications arise from a density dependent effect such as gluon recombination and are thus proportional to the local density. We calculate the dependence of charm and bottom quark production on impact parameter and show that density dependent modifications can lead to significant reductions in the heavy quark production cross sections in central relative to peripheral interactions.

(Submitted to Physical Review Letters.)

Experiments [1] have shown that the proton and neutron structure functions are modified by a nuclear environment. For momentum fractions  $x < 0.1$  and  $0.3 < x < 0.7$ , a depletion is observed in the nuclear parton distributions. The low  $x$ , or shadowing, region and the larger  $x$ , or EMC region, is bridged by an enhancement known as antishadowing for  $0.1 < x < 0.3$ . Recently, the entire characteristic modification as a function of  $x$  has been referred to as shadowing. Many theoretical explanations of the nuclear effect have been proposed. In most, the degree of modification depends on the local nuclear density. For example, if the modification is due to gluon recombination [2], then the degree of modification should depend directly on the local gluon density and hence on the spatial position of the interaction within the nucleus. Nuclear binding and rescaling models also predict that the structure function depends on the local density [3].

Most measurements of structure functions have used lepton or neutrino beams. Typically these experiments are insensitive to the location of the interaction within the nucleus so that the resulting structure functions are averaged over the entire nucleus. The Fermilab E745 collaboration studied  $\nu N$  interactions in a bubble chamber where the dark tracks indicated that the interaction occurred deep within the nucleon. They found that structure function does vary spatially, but had little direct sensitivity to the impact parameter [4].

This letter discusses the effects of spatially-dependent nuclear parton distributions on charm and bottom production cross sections as a function of impact parameter. Assuming that shadowing is proportional to the local nucleon density, we study the dependence of heavy quark production on the nucleon structure functions and the shadowing parameterization.

We show that the heavy quark production cross section changes significantly when this spatial dependence is considered. The variation with impact parameter is especially important because relatively peripheral collisions are often used as a baseline in searches for new phenomena in more central collisions [5]. Large impact parameter collisions tend to probe the nuclear surface where shadowing is rather weak while central collisions are also sensitive to structure functions at the nuclear core where nuclear modifications can be large.

The impact parameter of an event can be determined from the transverse energy pro-

duced in the event. The spatial dependence of shadowing on transverse energy production has already been considered [6]. In Au+Au collisions at  $\sqrt{s_{NN}} = 200$  GeV, the center of mass energy per nucleon pair, a typical calorimeter can measure impact parameters as large as  $b = 1.8R_A$  where  $R_A$  is the nuclear radius [7].

Heavy quark production in heavy ion collisions is dominated by gluon fusion [8,9]. At leading order (LO), charm and bottom quarks are produced in two basic processes:  $q\bar{q} \rightarrow Q\bar{Q}$  and  $gg \rightarrow Q\bar{Q}$  with  $Q = c$  and  $b$ . The LO cross section for a nucleus A with momentum  $P_A$  colliding with nucleus B with momentum  $P_B$  at an impact parameter  $b$  is then

$$E_Q E_{\bar{Q}} \frac{d\sigma_{AB}}{d^3p_Q d^3p_{\bar{Q}} d^2b d^2r} = \sum_{i,j} \int dz dz' dx_1 dx_2 F_i^A(x_1, Q^2, \vec{r}, z) F_j^B(x_2, Q^2, \vec{b} - \vec{r}, z') E_Q E_{\bar{Q}} \frac{d\hat{\sigma}_{ij}(x_1 P_A, x_2 P_B, m_Q, Q^2)}{d^3p_Q d^3p_{\bar{Q}}} . \quad (1)$$

where  $Q$  represents the produced heavy quark. Here  $i$  and  $j$  are the interacting partons in the nucleus and the functions  $F_i^A$  and  $F_j^B$  are the number densities of gluons, light quarks and antiquarks in each nucleus, evaluated at momentum fraction  $x$ , momentum scale  $Q^2$ , and location  $\vec{r}$ ,  $z$  in the two nuclei. The short-distance cross section,  $\hat{\sigma}_{ij}$ , is calculable as a perturbation series in the strong coupling constant  $\alpha_s(Q^2)$ , see Ref. [10].

These leading order calculations underestimate the measured charm production cross sections by a constant, usually called the  $K$  factor. A similar theoretical factor,  $K_{th}$ , is given by the ratio of the next-to-leading-order (NLO) cross section to the leading order result. The  $K$  factor is relatively independent of the quark  $p_T$ , pair invariant mass and rapidity distribution, and the parton density [11]. However, it can vary significantly with quark mass and beam energy.

Since this calculation is at leading order, we use the GRV 94 LO [12] nucleon parton distributions, evaluated with  $m_c = 1.3$  GeV,  $m_b = 4.75$  GeV and  $Q = m_T$  where  $m_T^2 = p_T^2 + m_Q^2$ . We also used the GRV 94 HO [12] with the same parameters and the MRS G distributions [14], evaluated with the same parameters for bottom and for charm,  $m_c = 1.2$  GeV and  $Q = 2m_T$ . The mass and scale parameters used with each set were chosen for their agreement with the  $Q\bar{Q}$  total cross section data.

We assume that the parton densities  $F_i^A(x, Q^2, \vec{r}, z)$  can be represented as the product of  $x$  and  $Q^2$  independent nuclear density distributions, position and  $A$  independent nucleon parton densities, and a shadowing function that contains the modification of the nuclear structure functions.

$$F_i^A(x, Q^2, \vec{r}, z) = \rho_A(s) S^i(A, x, Q^2, \vec{r}, z) f_i^p(x, Q^2) \quad (2)$$

$$F_j^B(x, Q^2, \vec{b} - \vec{r}, z') = \rho_B(s') S^j(B, x, Q^2, \vec{b} - \vec{r}, z') f_j^p(x, Q^2) ,$$

where  $f^p(x, Q^2)$  are the nucleon parton densities,  $s = \sqrt{r^2 + z^2}$  and  $s' = \sqrt{|\vec{b} - \vec{r}|^2 + z'^2}$ . In the absence of nuclear modifications of the structure functions (no shadowing),  $S^i(A, x, Q^2, \vec{r}, z) \equiv 1$ . The nuclear density is given by a Woods-Saxon distribution

$$\rho_A(s) = \rho_0 \frac{1 + \omega(s/R_A)^2}{1 + \exp[(s - R_A)/d]} \quad (3)$$

where electron scattering data from [13] is used to fix the parameters  $R_A$ ,  $d$ ,  $\omega$  and  $\rho_0$ .

The shadowing effect is studied with two parameterizations previously used to estimate the effect on heavy quark production without including spatial dependence [15]. The first,  $S_1(A, x)$  is based on fits to recent nuclear deep inelastic scattering data [16]. It treats the quark, gluon and antiquark functions equally without  $Q^2$  evolution. The second,  $S_2^i(A, x, Q^2)$  has separate modifications for the valence quarks, sea quarks and gluons and includes  $Q^2$  evolution [17].

To include the spatial dependence of shadowing, we assume that these modifications are proportional to the undisturbed local nuclear rest density, Eq. (3),

$$S_{\text{WS}}^i = S^i(A, x, Q^2, \vec{r}, z) = 1 + N_{\text{WS}}[S^i(A, x, Q^2) - 1] \frac{\rho(s)}{\rho_0} \quad (4)$$

where  $N_{\text{WS}}$  is a normalization constant chosen such that  $(1/A) \int d^3s \rho(s) S_{\text{WS}}^i = S^i$ . At large radii,  $s \gg R_A$ , medium modifications weaken so that in very peripheral interactions, nucleons behave as if they are in free space. At the center of the nucleus, the modifications are larger than the average value found in lepton scattering experiments. A second parameterization,  $S_{\text{R}}^i$ , based on the thickness of a spherical nucleus at the collision point [7], leads

to a slightly larger modification in the nuclear core. Because it assumes a sharp nuclear surface, for  $s \geq R_A$ ,  $S_R^i = 1$ , enhancing the shadowing at the center over that found with Eq. (4). Thus for surface nucleons, Eq. (4) predicts modifications half as strong as at the core while no further modifications are predicted with  $S_R^i$ . Other calculations assuming distinct shadowing effects in different nuclear orbitals [3] cannot be directly compared to our results.

With these ingredients, Eq. (1) can be used to find the charm and bottom cross sections as a function of impact parameter. Table 1 gives the total cross sections in nucleus-nucleus collisions integrated over impact parameter (in units of  $\mu\text{b}/\text{nucleon pair}$ ) for several cases. As a baseline for comparison we give the results with  $S = 1$  for GRV 94 HO and MRS G structure functions, followed by  $S = 1$ ,  $S_1$ , and  $S_2$  for GRV 94 LO. The theoretical  $K$  factors for each  $S = 1$  set are also included. We note that, with this normalization, the total cross section, integrated over all impact parameters, is unchanged when spatial dependence is included in  $S^i$ .

Although the spatial parameterizations are normalized to reproduce the impact-parameter integrated cross sections, the total cross section changes with impact parameter in heavy ion collisions. This effect is illustrated for the GRV 94 LO distributions in Figs. 1 and 2. To emphasize the role of the spatial dependence, the results are given relative to the  $S = 1$  cross section. Figure 1 presents the charm production ratios for collisions at LHC (Pb+Pb at  $\sqrt{s_{NN}} = 5.5$  TeV), RHIC (Au+Au at  $\sqrt{s_{NN}} = 200$  GeV) and the SPS (Pb+Pb at  $\sqrt{s_{NN}} = 17.3$  GeV) while Fig. 2 shows the bottom production ratios at LHC and RHIC.

Figure 1 shows that the nuclear effect increases with the collision energy. At RHIC and LHC, charm production occurs predominantly at momentum fractions  $x_i < 0.1$ , in the shadowing region, leading to a decrease in the cross sections for both  $S_1$  and  $S_2$ . In central collisions at the LHC, the cross section decreases by a nearly 50% while at RHIC the decrease is about 30%. In both cases, as the impact parameter increases, somewhat stronger shadowing is observed in central collisions when the spatial dependence is included while for impact parameters larger than  $R_A$  the shadowing decreases until the ratio begins to approach

unity for  $b > 2R_A$ . At the much lower SPS energy, charm production typically occurs in the antishadowing region. Since parameterization  $S_2$  includes stronger gluon antishadowing than  $S_1$ , the charm cross section is enhanced by 12% in central collisions when  $S_2$  is used while the nuclear effect with  $S_1$  is negligible. As the impact parameter increases, the enhancement decreases. Similar effects are seen with the other sets of parton distributions studied.

We note that these cross sections are integrated over the final-state kinematics and that, under certain kinematic conditions, the shadowing effect can be larger. Thus, the rapidity and  $p_T$  distributions of the produced quarks may exhibit a stronger shadowing spatial dependence, as shown in detail at RHIC energies in Ref. [7]. *E.g.* when  $y = 0$  for both charm quarks,  $x_1 = x_2$ , providing the cleanest determination of the magnitude of the nuclear modification.

Figure 2 shows the corresponding shadowing ratios for  $b\bar{b}$  production at LHC and RHIC. The heavier  $b$  quark probes larger values of  $x$  and  $Q^2$  than the charm quark at the same energies and thus exhibit a different shadowing pattern. At the lower  $Q^2$  of charm production, the scale-dependent shadowing parameterization  $S_2$  produces stronger gluon shadowing than  $S_1$  at LHC and RHIC. However, for  $b\bar{b}$  production, the  $Q^2$  dependence of  $S_2$  reduces the gluon shadowing with respect to  $S_1$ . Figure 1(a) shows an approximate 60% shadowing at  $b \approx 0$  with  $S_2$ , compared with 25% for  $b$  quarks in Fig. 2(a). Meanwhile calculations with  $S_1$  show little difference between charm and bottom production. This is because at the typical  $x$  values at LHC energies,  $\sim 4.7 \times 10^{-4}$  and  $1.7 \times 10^{-3}$  for  $c$  and  $b$  quarks respectively at  $y = 0$  and  $p_T = 0$ , nuclear shadowing has been seen to saturate [18] so that the larger  $x$  for  $b$  production has only a small effect on the  $Q^2$ -independent  $S_1$  parameterization. The lower energy of RHIC, where  $x \sim 0.013$  for charm and 0.048 for bottom with  $y = 0$  and  $p_T = 0$ , exhibits a larger difference between the heavy quarks, especially after  $Q^2$  evolution is considered. Over the kinematic range of the total cross section,  $b\bar{b}$  production results in a 2% enhancement in central collisions due to antishadowing for  $S_2$ . A 9% depletion is still observed for  $S_1$  without  $Q^2$  evolution. Although not shown, we note that at SPS energies,  $b$  production is predominantly in the EMC region of  $x$ , leading again to a depletion of bottom

production relative to that observed with no shadowing.

Our results show that using peripheral collisions as a baseline for comparison to central collisions can lead to significant errors if the spatial dependence of shadowing is not taken into account. At RHIC and LHC, the cross section is generally higher in peripheral collisions than might be expected without any spatial dependence of shadowing. Interestingly this effect is reversed at the SPS. We note however that the spatial dependence of the shadowing is not evident until  $b > 1.2R_A$ , requiring studies of peripheral collisions to determine the strength of the effect.

Similar impact parameter based effects should be observable in other hard processes such as  $J/\psi$  and Drell-Yan production [19]. The Drell-Yan pairs [20] are of special interest because they are produced by  $q\bar{q}$  interactions at leading order, in contrast to the gluon-dominated heavy quark production.

In conclusion, we have shown that introducing a very natural spatial dependence in nuclear shadowing changes the heavy quark production rates in heavy ion collisions, altering the expected relationship between central and peripheral collisions. This alteration could lead to a misinterpretation of the transverse energy dependence of certain quark-gluon plasma signatures due to the relationship between transverse energy and impact parameter.

V.E. and A.K. would like to thank the LBNL Relativistic Nuclear Collisions group for their hospitality and M. Strikhanov and V.V. Grushin for discussions and support. We also thank K.J. Eskola for providing the shadowing routines and for discussions. This work was supported in part by the Division of Nuclear Physics of the Office of High Energy and Nuclear Physics of the U. S. Department of Energy under Contract Number DE-AC03-76SF0098.

## REFERENCES

- [1] J.J. Aubert *et al.*, Nucl. Phys. **B293** 740, (1987); M. Arneodo, Phys. Rep. **240** 301, (1994).
- [2] L.V. Gribov, E.M. Levin, and M.G. Ryskin, Phys. Rep. **100** 1, (1983).
- [3] S. Kumano and F.E. Close, Phys. Rev. C **41**, 1855 (1990).
- [4] T. Kitagaki *et al.*, Phys. Lett. **214**, 281 (1988).
- [5] M.C. Abreu *et al.* (NA50 Collab.), Phys. Lett. **B410** (1997) 327, 337
- [6] K.J. Eskola, Z. Phys. C **51** 633 (1991).
- [7] V. Emel'yanov, A. Khodinov, S.R. Klein and R. Vogt, Phys. Rev. **C56**, 2726 (1997);  
V. Emel'yanov, A. Khodinov and M. Strikhanov, Yad. Fiz. **60**, 539 (1997) [Phys. of Atomic Nuclei, **60** 465, (1997)].
- [8] D.M. Alde *et al.*, Phys. Rev. Lett. **66** 133, (1991).
- [9] J.A. Appel, Ann. Rev. Nucl. Part. Sci. **42** 367, (1992).
- [10] R.K. Ellis, in *Physics at the 100 GeV Scale*, Proceedings of the 17th SLAC Summer Institute, Stanford, California, 1989, edited by E.C. Brennan (SLAC Report No. 361, Stanford, 1990).
- [11] P.L. McGaughey *et al.*, Int. J. Mod. Phys. **A10** 2999, (1995).
- [12] M. Glück, E. Reya, and A. Vogt, Z. Phys. **C67** 433, (1995).
- [13] C.W. deJager, H. deVries, and C. deVries, Atomic Data and Nuclear Data Tables **14** 485, (1974).
- [14] A.D. Martin, R.G. Roberts and W.J. Stirling, Phys. Lett. **B354** 155, (1995).
- [15] S. Gavin, P.L. McGaughey, P.V. Ruuskanen and R. Vogt, Phys. Rev. **C54** 2606, (1996).



- [16] K.J. Eskola, J. Qiu, and J. Czyzewski, private communication.
- [17] K.J. Eskola, Nucl. Phys. **B400** 240, (1993).
- [18] M.R. Adams *et al.*, Phys. Rev. Lett. **68** 3266, (1992).
- [19] V. Emel'yanov, A. Khodinov, S.R. Klein and R. Vogt, in preparation.
- [20] P. Castorina and A. Donnachie, Z. Phys. C **49**, 481 (1991).

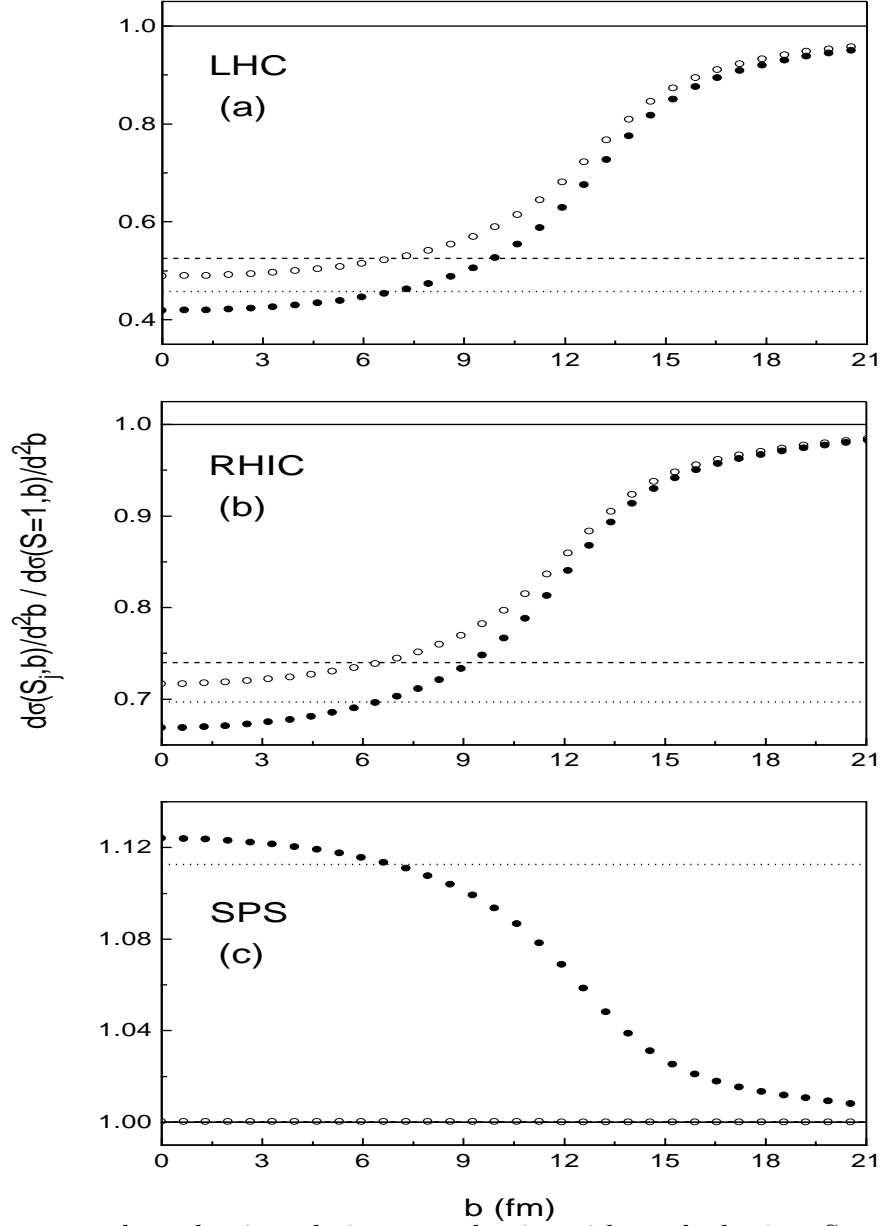


FIG. 1. Charm quark production relative to production without shadowing,  $S = 1$ , as a function of impact parameter. The dashed and dotted lines show the effect with shadowing but without spatial dependence for  $S_1$  and  $S_2$  respectively. The spatial dependence is illustrated for  $S_{1ws}$  (open circles) and  $S_{2ws}$  (filled circles). The results are shown for (a) Pb+Pb collisions at the LHC with  $\sqrt{s_{NN}} = 5.5$  TeV, (b) Au+Au collisions at RHIC with  $\sqrt{s_{NN}} = 200$  GeV and (c) Pb+Pb collisions at the CERN SPS with  $\sqrt{s_{NN}} = 17.3$  GeV.

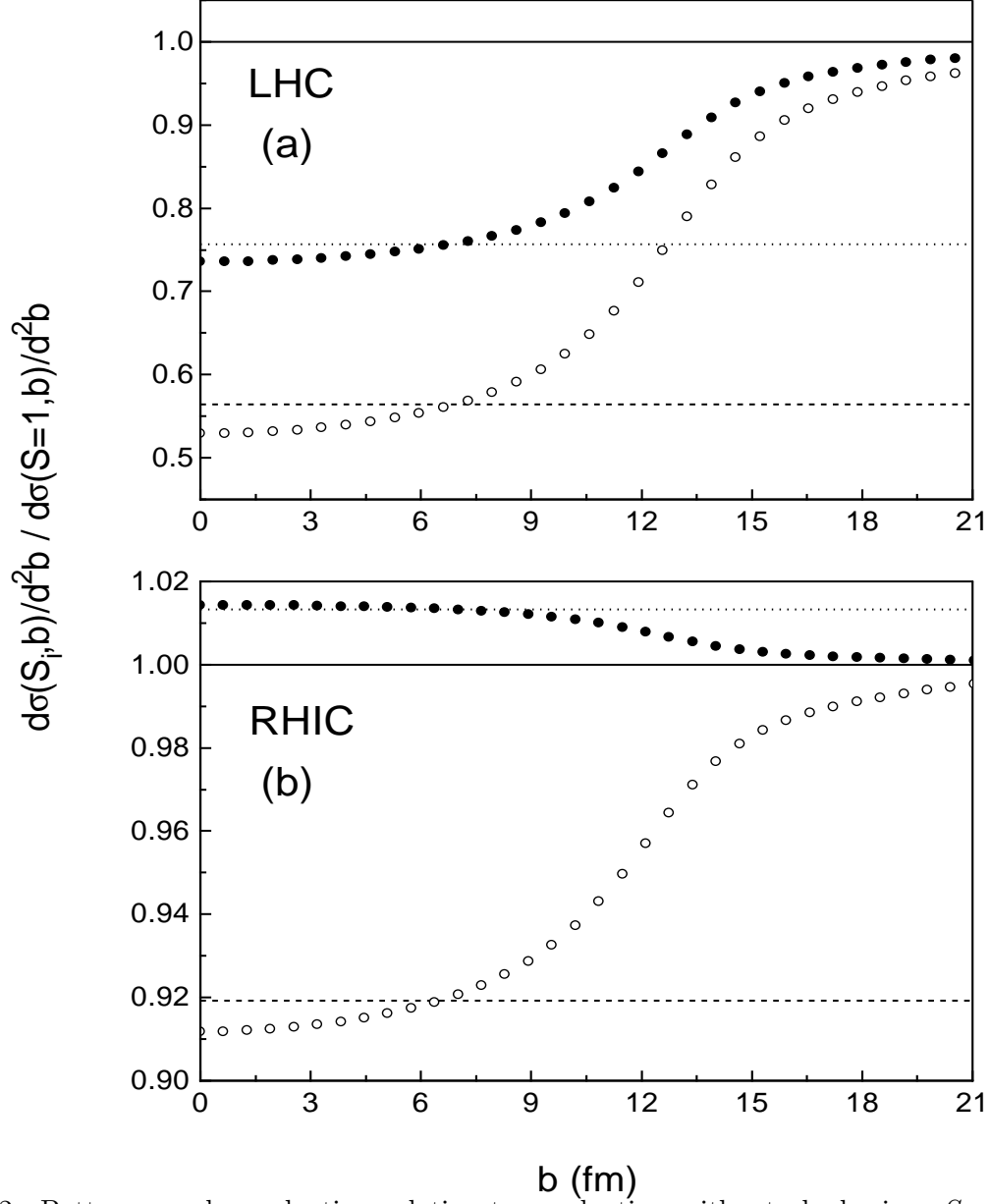


FIG. 2. Bottom quark production relative to production without shadowing,  $S = 1$ , as a function of impact parameter. The dashed and dotted lines show the effect with shadowing but without spatial dependence for  $S_1$  and  $S_2$  respectively. The spatial dependence is illustrated for  $S_{1WS}$  (open circles) and  $S_{2WS}$  (filled circles). The results are shown for (a) Pb+Pb collisions at the LHC with  $\sqrt{s_{NN}} = 5.5$  TeV and (b) Au+Au collisions at RHIC with  $\sqrt{s_{NN}} = 200$  GeV.

# TABLES

$\sqrt{s_{NN}}$		MRS G		GRV 94 HO		GRV 94 LO			
(GeV)	$Q\bar{Q}$	$\sigma(S=1)$	$K_{\text{th}}$	$\sigma(S=1)$	$K_{\text{th}}$	$\sigma(S=1)$	$K_{\text{th}}$	$\sigma(S_1)$	$\sigma(S_2)$
17.3	$c\bar{c}$	1.53	2.85	1.80	2.35	1.85	2.36	1.85	2.06
200	$c\bar{c}$	138	2.31	107	2.35	174	2.46	129	121
200	$b\bar{b}$	0.693	1.87	0.702	1.84	0.940	1.89	0.866	0.953
5500	$c\bar{c}$	5622	2.10	2130	2.77	7440	2.69	3910	3410
5500	$b\bar{b}$	93.7	1.78	85.7	1.71	212	1.80	120	160

TABLE I. Leading order  $c\bar{c}$  and  $b\bar{b}$  total cross sections, in units of  $\mu\text{b}$  per nucleon pair, integrated over all impact parameters, for the MRS G, GRV 94 HO and GRV 94 LO parton distribution as well as the theoretical  $K$  factors ( $K_{\text{th}} = \sigma_{\text{NLO}}/\sigma_{\text{LO}}$ ) for  $S = 1$ . The cross sections including shadowing are also given for the GRV 94 LO distributions. The quark masses and the scale parameters are described in the text.